Mode selective photodissociation dynamics in V$^+$(OCO)

Murat Citir and Ricardo B. Metz[a)]

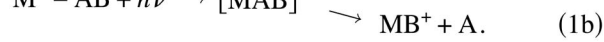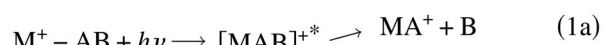*Department of Chemistry, University of Massachusetts Amherst, Amherst, Massachusetts 01003, USA*

The electrostatic V$^+$(OCO) complex has a vibrationally resolved photodissociation spectrum in the visible. Photodissociation produces V$^+$+CO$_2$ (nonreactive pathway) and VO$^+$+CO (reactive pathway). Production of VO$^+$ is energetically favored, but spin forbidden. One-photon dissociation studies confirm mode selectivity observed by Lessen *et al.* [J. Chem. Phys. **95**, 1414 (1991)]: excitation of one quantum of rocking motion enhances VO$^+$ production by >30%. Branching ratio measurements in one-photon dissociation are extended to higher energy. The effect of OCO antisymmetric stretch vibrations on reactivity is investigated using vibrationally mediated photodissociation, in which the OCO antisymmetric stretch is excited at 2390.9 cm^{-1}. Vibrationally excited molecules are then dissociated in the visible. Seven vibronic bands are investigated, involving the antisymmetric stretch alone and in combination with the CO$_2$ bend, the V$^+$(OCO) stretch and rock. Exciting the antisymmetric stretch leads to a ~15% increase in the reactive VO$^+$ channel, compared to other states at similar energy. Combination bands involving the antisymmetric stretch all show slightly higher reactivity. Electronic structure calculations were performed to characterize the dissociation pathways and excited electronic states of V$^+$(OCO). The geometries of reactants, products, and transition states and relative energies of quintet and triplet states were determined using hybrid density functional theory; energies were also calculated using the coupled cluster with single, double and perturbative triple excitations method. In addition, time-dependent density functional theory calculations were performed to predict the excited electronic states of quintet and triplet V$^+$(OCO). Spin-orbit coupling of quintet states to triplet states was calculated and used to compute intersystem crossing rates, which reproduce many of the observed mode selective trends. The V$^+$−OCO stretch and OCO antisymmetric stretch appear to enhance reactivity by increasing the intersystem crossing rate. © *2008 American Institute of Physics.*
[DOI: 10.1063/1.2818564]

INTRODUCTION

Influencing the course of a reaction to promote a desired product channel is a long-standing goal of chemistry. Compared to a bimolecular reaction, photoinitiating the reaction from an isolated, weakly bound reactant cluster provides greater control over the reaction, as reactant orientation, angular momentum, and energy are constrained. In addition, specific vibrational motions in the cluster can be photoexcited and any chemistry dependent on this motion revealed. During the path of a branched reaction the species involved must at some point along the reaction coordinate "choose" which path to follow. If at or near this decision point the complex is selectively excited along a particular vibrational mode, the branching ratios for the reaction may change. Control of ion-molecule reactions is experimentally attractive because the reactant complex is much more strongly bound than neutral van der Waals complexes and because the products and their branching ratio can readily be measured using mass spectrometry. If we can identify and excite a vibration in [MAB]$^{+*}$ that corresponds to the desired motion, then we

may be able to control the products of the corresponding M^{+*}+AB reaction, influencing the relative production of MA$^+$+B and MB$^+$+A,

$$\text{M}^+ - \text{AB} + h\nu \longrightarrow [\text{MAB}]^{+*} \begin{array}{l} \nearrow \quad \text{MA}^+ + \text{B} \qquad (1a) \\ \searrow \quad \text{MB}^+ + \text{A}. \qquad (1b) \end{array}$$

V$^+$(OCO) is a particularly interesting system in which to investigate mode selectivity, as it is a small molecule with two chemically district pathways at similar energies,

$$\text{V}^+(\text{OCO}) + h\nu$$

$$\begin{array}{l} \nearrow \quad \text{V}^+(^5D) + \text{CO}_2(^1\Sigma^+) \quad \Delta H = 0.75 \pm 0.04 \text{ eV} \quad (2a) \\ \searrow \quad \text{VO}^+(^3\Sigma) + \text{CO}(^1\Sigma^-) \quad \Delta H = 0.21 \pm 0.10 \text{ eV}. \quad (2b) \end{array}$$

V$^+$ forms a linear, electrostatic complex with CO$_2$, and V$^+$(OCO) is calculated to have a $^5\Sigma$ or $^5\Delta$ ground state.[1,2] Vibrational spectroscopy confirms that V$^+$(OCO) is linear.[1] Dissociation via the reactive pathway (2b) is energetically favored, but is spin forbidden. Lessen *et al.* obtained a vibrationally resolved photodissociation spectrum of V$^+$(OCO) in the visible region.[3] Dissociation occurs through both the reactive (2b) and nonreactive (2a) channels. They observed an

interesting mode selectivity. The VO^+/V^+ branching ratios for states with no vibrational excitation in the electronically excited $V^+(OCO)$ and excitation of one quantum of $V^+(OCO)$ stretch or CO_2 bend are identical. However, excitation of one quantum of the rocking motion enhances the relative VO^+ production by 50%.

In a simple, collinear picture, the reaction coordinate for the reactive channel should be similar to the OCO antisymmetric stretch vibration. So, exciting this vibration should also enhance reactivity, but progressions in this stretch were not observed in the spectrum, due to small Franck-Condon factors. Recently, we measured the OCO antisymmetric stretch frequency in the ground electronic state of $V^+(OCO)$ $\nu_1''=2392$ cm^{-1} using vibrationally mediated photodissociation.[1] In this work, we use vibrationally mediated photodissociation (VMP) to study how the OCO antisymmetric stretch and combinations of antisymmetric stretch with other vibrations affect the mode selectivity of reaction 2. IR absorption prepares molecules with one quantum of antisymmetric OCO stretch. A visible photon promotes the molecules to a predissociative electronic state, with one quantum of OCO antisymmetric stretch excitation, alone or in combination with the V^+-(OCO) stretch and rock, and the CO_2 bend.

EXPERIMENTAL APPROACH

Vibrationally mediated photodissociation of $V^+(OCO)$ was studied on a dual time-of-flight reflectron photofragment spectrometer which has been described in detail previously.[4,5] Vanadium cations are produced in a standard laser ablation source. The frequency-doubled output of a pulsed Nd:YAG (YAG denotes yttrium aluminum garnet) laser operating at 20 Hz repetition rate is loosely focused onto a rotating and translating vanadium rod (Sigma-Aldrich, 99.98% pure). Ablated V^+ ions react with a gas mixture of ~0.08% carbon dioxide (99.98% pure) in helium (99.98% pure) to produce $V^+(OCO)_n$. Ions produced in the source undergo supersonic expansion into vacuum, producing electronically and vibrationally cold ions with rotational temperatures of ~12 K.[1] The molecular beam is skimmed, and ions are extracted along the beam axis using a pulsed electric field, accelerated to 1800 V kinetic energy and rereferenced to ground potential prior to entering the time-of-flight mass spectrometer. Ions are photodissociated at the turning point of the reflectron. Fragment ions are detected by a dual 40 mm dia. microchannel plate detector and the signal is amplified and collected using a 500 MHz digital oscilloscope. Fragment ions and their branching ratios are measured using *difference spectra*, the difference between time-of-flight spectra obtained with the laser unblocked and blocked. *Photodissociation spectra* are obtained by measuring signal in a particular fragment ion channel as a function of wavelength using a gated integrator and normalizing to parent ion signal and laser power.

In the VMP studies, ions are vibrationally excited with an IR laser. A visible laser then promotes vibrationally excited molecules to a predissociative excited electronic state. An IR optical parametric oscillator/optical parametric ampli-
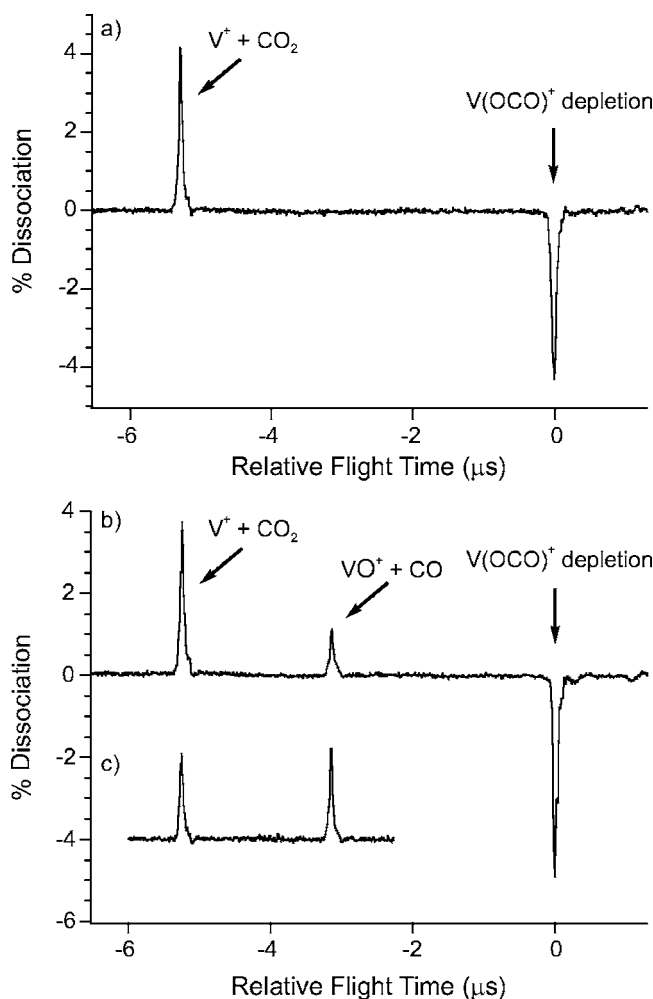

FIG. 1. Difference spectra obtained from photodissociation of $V^+(OCO)$ (a) in the near-IR band at 7300 cm^{-1}, (b) at the origin of the visible band (15801 cm^{-1}), and (c) from molecules with one quantum of OCO antisymmetric stretch vibration in the excited electronic state, produced by exciting the antisymmetric stretch ν_1 at 2390.9 cm^{-1}, then the 1_1^1 band at 15 777.1 cm^{-1}. Figure 1(c) has been multiplied by a factor of 4.

fier (OPO/OPA) (Laser Vision) pumped by an injection-seeded Nd:YAG laser produces light in the midinfrared region. The IR laser system uses a combination of a 532 nm pumped OPO and a 1064 nm pumped OPA. It is tunable from 2100 to >4000 cm^{-1} in the mid-IR, producing 3 mJ/pulse near 2400 cm^{-1}, with 0.2 cm^{-1} linewidth. It also produces 3–9 mJ/pulse from 6050–7425 cm^{-1} in the near IR. The visible laser system is a Nd:YAG pumped dye laser (Continuum) with <0.08 cm^{-1} linewidth. The mid-IR laser wavelengths are calibrated using the photoacoustic spectrum of methane.[6] The dye laser is calibrated using the absorption spectrum of I_2.[7] The delay between the IR and visible lasers is ~40 ns.

RESULTS

One-photon dissociation

In the near IR, $V^+(OCO)$ has a complex photodissociation spectrum.[1] Throughout this region, photodissociation occurs solely via production of V^+ (nonreactive channel), as shown in Fig. 1(a). $V^+(OCO)$ has a second absorption band
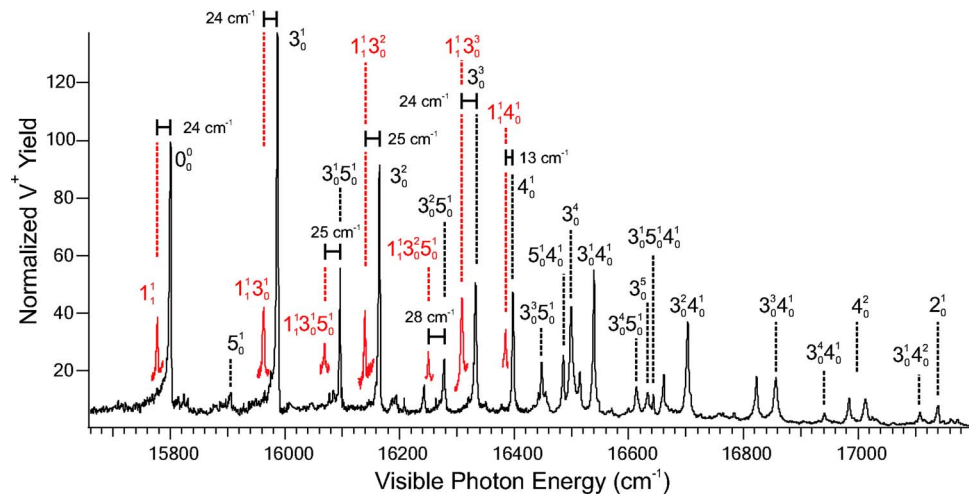
FIG. 2. (Color online) Photodissociation spectrum of V$^+$(OCO), with assignments (black). Insets and assignments in red show the photodissociation spectrum of molecules excited with one quantum of OCO antisymmetric stretch, ν_1'' at 2390.9 cm^{-1}. Their intensities have been multiplied by a factor of 2. The shifts show that ν_1' (excited state) lies $\sim$24 cm^{-1} below ν_1'' (ground state), and that there is a small amount of vibrational cross anharmonicity.

in the visible region, with sharp, well resolved vibronic features. Photodissociation in this band leads to production of both V$^+$ and VO$^+$, as shown in Fig. 1(b).

Figure 2 shows the photodissociation spectrum of V$^+$(OCO) in the visible region. This spectrum was previously observed by Lessen *et al.*[3] The origin lies at 15 801 cm^{-1}. There are progressions in several excited state vibrations, the V$^+$-(OCO) stretch (ν_3'=186 cm^{-1}), the OCO bend (ν_4'=597 cm^{-1}), and the V$^+$-(OCO) rock (ν_5' =105 cm^{-1}), all in agreement with the earlier study.[3] We also observe a weak transition due to the OCO symmetric stretch, which gives ν_2'=1340 cm^{-1}. Using vibrationally mediated photodissociation, we previously[1] measured the OCO antisymmetric stretch ν_1'=2368 cm^{-1}, so all vibrational frequencies in the excited electronic state of V$^+$(OCO) have been measured. Using difference spectra, we determine the branching ratio of the reactive VO$^+$ channel to the nonreac-

tive V$^+$ channel at 51 vibronic peaks in the visible band. These measure the influence of the V$^+$-(OCO) stretch and rock, CO$_2$ bend, and combinations of these motions, on the dissociation pathway. The results are shown in Fig. 3. Detailed results and assignments are in Table S1 of Ref. 8. Our results on the branching ratios generally agree with those previously obtained by Lessen *et al.* One quantum of V$^+$-(OCO) rock (ν_5') enhances the reactive channel, while one quantum of V$^+$-(OCO) stretch (ν_3') or CO$_2$ bend (ν_4') slightly decreases it. We also find significant enhancement ($\sim$70%) of reactivity when exciting $3\nu_3'+\nu_5'$ which lies only 50 cm^{-1} above ν_4', a result that was not reported earlier, presumably due to the low total photodissociation cross section for this peak. Overall, reactivity for one-photon dissociation generally increases with energy, up to energies of $\sim$17 000 cm^{-1} and a VO$^+$/V$^+$ ratio of $\sim$0.95, then slightly decreases at higher energy.
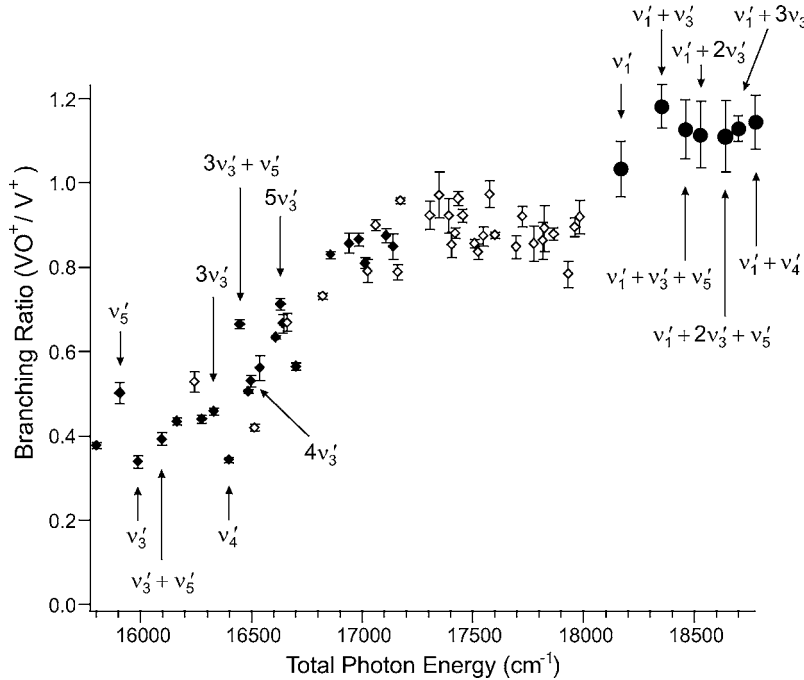

FIG. 3. Mode selectivity in photodissociation of V$^+$(OCO). The ratio of the reactive (VO$^+$+CO) to nonreactive (V$^+$+CO$_2$) product is measured at the peaks of the vibronic bands shown in Fig. 2. The diamonds show bands accessed by one-photon excitation, data obtained by vibrationally mediated photodissociation exciting the OCO antisymmetric stretch is shown in circles. Filled symbols correspond to assigned peaks (assignments in Fig. 2 and Table S1).

Vibrationally mediated photodissociation

We recently measured the OCO antisymmetric stretch frequency ν_1'' in the ground electronic state of V$^+$(OCO) using two techniques: photodissociation depletion spectroscopy and vibrationally mediated photodissociation.[1] We find ν_1'' =2392 cm^{-1}, which is 43 cm^{-1} blueshifted from the value in isolated CO$_2$. Setting the IR laser to the peak of the P branch of the ν_1 band at 2390.9 cm^{-1} and tuning the visible laser in the vicinity of the vibronic origin band reveals a new peak at 15 777 cm^{-1} (Fig. 2). This peak is due to the $\nu_1'=1 \leftarrow \nu_1''=1$ sequence band. The 24 cm^{-1} shift to the red of the origin gives $\nu_1'=2392-24=2368$ cm^{-1}.

In general, VMP experiments have been used to measure the spectroscopy of regions of the potential energy surface of the excited state that are not Franck-Condon accessible from the ground state and to show how different vibrations affect the photodissociation dynamics.[9–12] In this case, IR excitation of the OCO antisymmetric stretch (ν_1'') allows us to access excited state vibronic bands with $\nu_1'=1$ and to measure how antisymmetric stretch excitation affects the dissociation dynamics. Figure 1(c) shows the difference mass spectrum obtained after exciting the $\nu_1'=1 \leftarrow \nu_1''=1$ band. This was obtained by taking the difference between time-of-flight mass spectra with the IR laser blocked and unblocked. The visible laser was always unblocked. Uncertainties in the VO$^+$/V$^+$ branching ratio are larger in the VMP experiments than in the one-photon measurements, as the total fragment signal is smaller, and there is always fragment signal from the visible laser alone. Comparison of Figs. 1(b) and 1(c) clearly shows that antisymmetric stretch excitation enhances the yield of the reactive VO$^+$ product.

We excited several different combination bands involving the OCO antisymmetric stretch, as shown in Fig. 2. At each peak, we measured the relative amounts of reactive (VO$^+$) and unreactive (V$^+$) products produced by photodissociation of V$^+$(OCO). Our experimental results are summarized in Fig. 3 (filled circles) and in Table S1 of Ref. 8. Exciting the OCO antisymmetric stretch enhances the VO$^+$ yield by almost a factor of 3, compared to the yield for the ground vibrational state. Exciting combination bands of antisymmetric stretch with several other vibrations increases the VO$^+$ yield a bit more, but combination bands involving the antisymmetric stretch all give similar branching ratios. Excitation of the antisymmetric stretch slightly enhances the reactivity, even when compared with other vibrational states at similar energy. Figure 3 shows that, above ~17 000 cm^{-1} the branching ratio for states accessed by one-photon excitation reaches a plateau at ~0.9 and may decrease slightly at higher energy. Compared to this value, states produced by vibrationally mediated photodissociation exciting the OCO antisymmetric stretch show enhanced reactivity of ~15% for ν_1' and ~25% for combination bands involving ν_1'.

Electronic structure calculations

To characterize V$^+$(OCO), its excited electronic states, and dissociation pathways we did three types of calculations. We first calculated the geometries and relative energies of quintet and triplet V$^+$(OCO) and OV$^+$CO and the transition state connecting them. We then calculated excited electronic states of quintet and triplet V$^+$(OCO). Finally, we calculated the spin-orbit coupling between the quintet and triplet states.

Density functional theory is used for geometry optimization and frequency calculations. All geometries are optimized using Becke's three-parameter hybrid functional[13] combined with the Lee, Yang, and Parr[14,15] (LYP) correlation functional (B3LYP) with the 6-311+G(d) basis set. To obtain improved energies, single point calculations have been performed at the B3LYP/6-311+G(d) equilibrium geometries, using the coupled cluster with single, double and perturbative triple excitations [CCSD(T)] method.[16] Calculations were also carried out with the larger 6-311+G($3df$) basis set which includes three d and one f polarization function on C and O and three f and one g polarization function on V. At each optimized stationary point, a vibrational analysis was performed to determine its character (minimum or saddle point) and to evaluate the zero point vibrational energy correction at B3LYP/6−311+G(d). For the transition state structure optimizations, we used the Synchronous transit-guided quasi-Newton[17,18] (STQN) method. These calculations were carried out with the GAUSSIAN 03 package.[19]

Geometries calculated at the B3LYP/6−311+G(d) level are quite good. For example, calculated r_e=1.538 Å for VO$^+$ compared to experiment r_o=1.561±0.002 Å (Ref. 20) and C–O bond lengths of 1.128 Å in CO and 1.161 Å in CO$_2$ agree with experiment to 0.001 Å. The V$^+$(OCO) ground state is calculated to be $^5\Delta$, with bond lengths of 2.116 Å (V–O$_1$), 1.178 Å (O$_1$–C), and 1.142 Å (C–O$_2$). Binding to V$^+$ lengthens the adjacent C–O bond by 0.017 Å and shortens the distant bond by a similar amount. Orbitals and electronic occupancies are shown in Fig. 4. The 5π, 13σ, 1δ, and 14σ are primarily $3d$ and $4s$ vanadium orbitals.

To evaluate the reliability of the B3LYP and CCSD(T) energies we compare calculated and experimental excitation energies of V$^+$ and bond dissociation energies for several vanadium compounds (Table I). All energies are calculated at the B3LYP/6-311+G(d) geometry and include zero point energy at the B3LYP/6-311+G(d) level. The splitting between the ground ($^5D, 3d^4$) and lowest triplet ($^3F, 3d^34s^1$) states of V$^+$ is fairly well reproduced by B3LYP calculations. Our B3LYP results are very similar to those Sicilia and Russo obtained with B3LYP/DZVP and B3LYP/TZVP.[21] The calculated CCSD(T) splitting is too low and is strongly dependent on the basis set. Several groups have calculated D_0(V$^+$−O) using density functional theory as well as CCSD(T), complete active space self consistent field (CASSCF), multiconfiguration self consistent field (MCSCF), multireference average coupled-pair functional (MRACPF), multireference singles and doubles configuration interaction (MR-SDCI), and multireference second order Møller-Plesset (MRMP).[22–26] Our DFT and CCSD(T) results agree with the earlier values, but the calculated values are consistently lower than experiment.[20,27–31] A recent multireference average coupled-pair functional (MR-ACPF) study obtained a value of 5.98 eV for D_0(V$^+$−O), but this required developing very large correlation consistent basis sets and extrapolating to the basis set limit.[22] Accurately reproducing the quintet-triplet splitting and VO$^+$ bond strength with
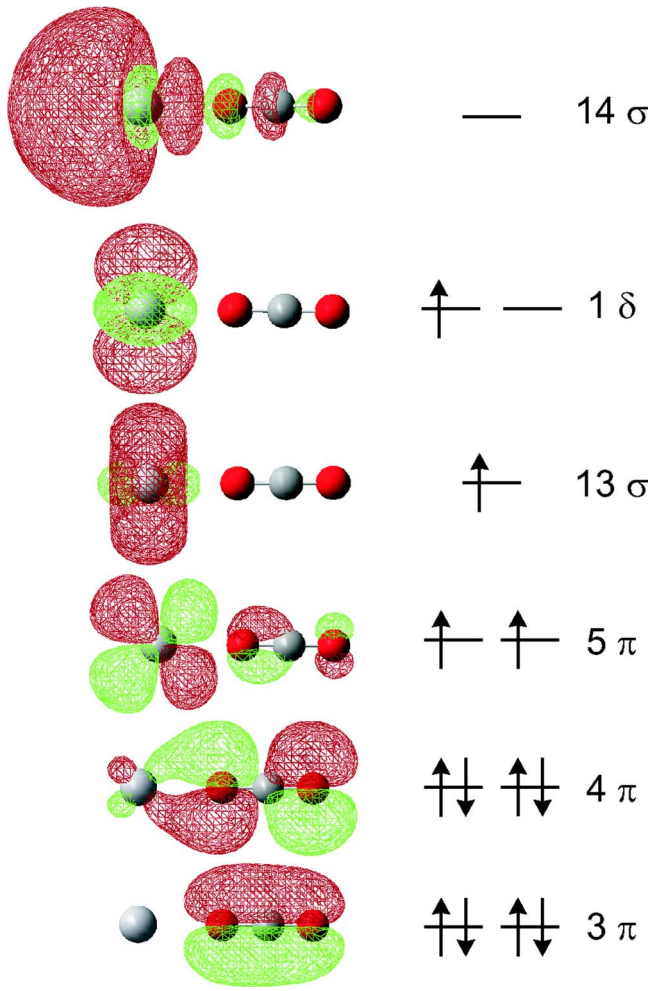
FIG. 4. (Color online) Molecular orbitals and electron occupancy of quintet $V^+(OCO)$ ($^5\Delta$) calculated at the B3LYP/6-311+G($3df$) level.

CCSD(T) will likely require substantially larger basis sets than are currently practical for $V^+(OCO)$ and its isomers. Calculated values for $D_0(V^+-OCO)$ and $D_0(OV^+-CO)$ are in excellent agreement with the guided ion beam experiments,[31] particularly the CCSD(T) results; they also show a much smaller dependence on basis set than $D_0(V^+-O)$.

Figure 5 shows the calculated potential energy surface for the V^++CO_2 reaction at the CCSD(T)/6-311+G($3df$)

level. Energies calculated with the smaller basis set and at the B3LYP level are also shown in Table II and the geometries of stationary points are in Table III. As noted earlier, the energies of the minima have been calculated previously, but this is the first calculation of the barrier to insertion. The global minimum of the PES is the triplet state of OV^+CO (Min2). This agrees with the calculation of Sodupe *et al.*[2] and with the guided ion beam experiment,[31] which places triplet OV^+CO 0.84±0.14 eV below quintet $V^+(OCO)$. Our calculations predict that there is a barrier for V^+ (^5D) to react with CO_2 to produce VO^+ ($^3\Sigma$)+CO. Calculations with the larger basis set predict a smaller barrier, so the size of the barrier is likely not converged with respect to basis set. The prediction of a barrier to reaction agrees with a recent selected ion flow tube (SIFT) study[32] which finds that V^+ does not react with CO_2 at thermal energies. Earlier guided ion beam (GIB) experiments[31] found that V^+ reacts with CO_2 at low collision energy and that the reaction cross section drops with collision energy, indicating a reaction with no barrier. However, the SIFT results suggest that the VO^+ observed in the GIB experiments may have been due to trace O_2 impurity, a possibility also raised in the original paper.[31] Guided ion beam experiments find that collisions of $V^+(OCO)$ with Xe lead exclusively to V^+, with no VO^+ observed at collision energies below 9 eV and VO^+/V^+ ratios below 0.03 at higher energies. The small amount of VO^+ product is in sharp contrast to what is found in the photodissociation studies, where $VO^+/V^+ > 0.3$ throughout the visible band. The reasons for this difference in reactivity will be explored, using the calculations described above of stationary points on the potential energy surfaces for the reaction, as well as calculations of excited quintet and triplet states.

Our studies of the vibrational and electronic spectroscopy of $V^+(OCO)$ probe the ground state of the molecule, as well as two excited electronic states, at ~6000 and ~15 800 cm^{-1}, respectively.[1] We have used time-dependent density functional theory (TD-DFT) to calculate excited electronic states of $V^+(OCO)$. Calculations of excited electronic states of coordinatively unsaturated transition metal systems are challenging, due to the large number of low-lying electronic states. In general, TD-DFT gives excitation energies for transitions involving valence states with surpris-

TABLE I. Calculated and experimental excitation energy and bond dissociation energies for vanadium containing systems. All values are in eV. Calculations are single-point energies at the optimized B3LYP/6-311+G(d) geometry and include zero point energy at the B3LYP/6-311+G(d) level.

	B3LYP		CCSD(T)		
Property	6-311+G(d)	6-311+G($3df$)	6-311+G(d)	6-311+G($3df$)	Experiment
$V^+(^3F-^5D)$	0.94	0.93	0.44	0.56	1.08[a]
$D_0(V^+-O)$	5.51	5.63	5.22	5.52	5.85±0.15,[b] 5.99±0.09[c]
$D_0(V^+-OCO)$	0.94	0.95	0.74	0.75	0.75±0.04[d]
$D_0(OV^+-CO)$	1.08	1.13	0.93	0.99	1.05±0.10[d]

[a]Averaged over spin-orbit levels (Ref. 34).
[b]References 26–28.
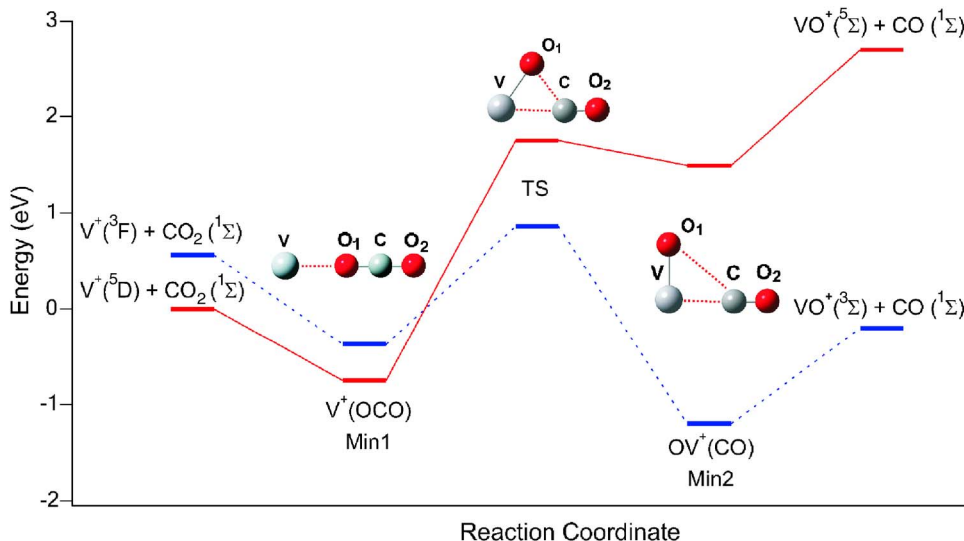[c]Based on $D_0(V^+-O)=D_0(V-O)+IE(V)-IE(VO)$ (Refs. 19 and 29).
[d]Reference 30.

FIG. 5. (Color online) Calculated potential energy surface for the V+ +CO₂ reaction. Energies are at the CCSD(T)/6-311+G(3df) level, at the B3LYP/6-311+G(d) geometry and include zero point energy at the B3LYP/6-311+G(d) level.

ingly good accuracy,[33,34] providing an efficient alternative to sophisticated wave function based approaches.

As $V^+(OCO)$ is an electrostatically bond complex, its electronic states can be correlated to those of V^+, so we first perform TD-DFT calculations to evaluate the ability of different functionals (B3LYP, B3PW91, B3P86, B98, BHandHLYP) and basis sets (6-311+G(d), 6-311+G(3df), CEP-121G, TZVP, SDD) to accurately predict excited states of V^+. Experimentally, V^+ has a ^5D ground state, with a $3d^4$ electronic configuration. The two lowest excited quintet states are $3d^34s$ (^5F) at 0.34 eV and $3d^34s$ (^5P) at 1.67 eV (energies are the weighted average of spin-orbit states).[35] All of the functionals tested give an excitation energy for the ^5P state that is too low, and several split the ^5F into nondegenerate states. Results are given in Table S2 of Ref. 8.

Overall, the BHandHLYP functional with the 6-311 +G(3df) basis set performed best, predicting the ^5F state at 0.48 eV and ^5P at 1.34 eV and we used it for subsequent calculations on $V^+(OCO)$. The optimized geometry of quintet $V^+(OCO)$ with BHandHLYP/6-311+G(3df) is $r(V-O_1)=2.114$ Å, $r(O_1-C)=1.163$ Å, and $r(C-O_2)=1.126$ Å, which is very similar to the B3LYP/6-311 +G(d) geometry. We then performed TD-DFT calculations

on quintet and triplet $V^+(OCO)$. The resulting adiabatic potential curves along the $V^+-(OCO)$ stretch are shown in Fig. 6. At each $V^+-(OCO)$ distance $r(V-O_1)$, all other bond lengths are optimized for the ground state of the linear complex, for each spin state. We also carried out TD-DFT calculations to study the potential for the $V^+-(OCO)$ rock. We fix the V–C bond length and the geometry of the OCO ligand to their values at the quintet minimum and scan the $V-O_1-C$ angle (θ) from 0° to 90° (Fig. 7). Focusing first on the quintet states in Fig. 6 (shown with symbols), the three lowest states correlate to ground state V^+ ($3d^4$, ^5D). Interaction with the ligand causes the degenerate atomic state to split into $^5\Delta$, $^5\Sigma$, and $^5\Pi$ states, based on the orientation of the unoccupied d orbital (see Fig. 4). All three states have a minimum at $r(V-O_1)=2.11-2.16$ Å, with a linear equilibrium geometry. The next two quintet states correlate to V^+ ($3d^34s$, ^5F). They are more weakly bound, and have longer metal-ligand bond lengths $r(V-O_1)\approx2.5$ Å. This is to be expected, as V^+ states with a $4s$ electron will have weaker electrostatic binding, due to repulsion between the ligand and the $4s$ electron. Transitions to one or both of these states are responsible for the photodissociation we previously observed[1] from 6050 to

TABLE II. Energies of stationary points on the V^++CO₂ potential energy surface calculated using the B3LYP and CCSD(T) methods. All energies are in eV, relative to $V^+(^5D)$+CO₂. Single point energies are calculated at the optimized B3LYP/6-311+G(d) geometry and include zero point energy at the B3LYP/6-311+G(d) level.

	B3LYP		CCSD(T)	
Species	6-311+G(d)	6-311+G(3df)	6-311+G(d)	6-311+G(3df)
$V^+(^5D)$+CO₂($^1\Sigma^+$)	0.00	0.00	0.00	0.00
$V^+(^3F)$+CO₂($^1\Sigma^+$)	0.94	0.92	0.44	0.56
$V^+(OCO)$, Min1 ($^5A''$)	−0.94	−0.95	−0.74	−0.75
$V^+(OCO)$, Min1 ($^3A'$)	−0.10	−0.13	−0.43	−0.37
TS ($^5A''$)	1.74	1.67	1.79	1.76
TS ($^3A''$)	0.81	0.71	0.99	0.86
$OV^+(CO)$, Min2 ($^5A''$)	1.50	1.46	1.46	1.50
$OV^+(CO)$, Min2 ($^3A''$)	−1.12	−1.15	−1.24	−1.19
$VO^+(^5\Sigma)$+CO($^1\Sigma^-$)	2.74	2.73	2.59	2.70
$VO^+(^3\Sigma)$+CO($^1\Sigma^-$)	−0.03	−0.02	−0.31	−0.20

TABLE III. Calculated B3LYP/6-311+G(d) geometries of the V$^+$(OCO) and OV$^+$(CO) minima, and of the transition state between them, for the lowest quintet and triplet states. Bond lengths (R) in Å and angles ($\angle$) in degrees.

Structure	State	$R(V-O_1)$	$R(O_1-C)$	$R(C-O_2)$	$R(V-C)$	$\angle V-O_1-C$	$\angle O_1-C-O_2$	$\angle O_1-V-C$
Min1	Quintet	2.116	1.178	1.142	3.294	180.0	180.0	⋯
Min1	Triplet	2.096	1.178	1.141	3.274	180.0	180.0	⋯
Min2	Quintet	1.844	2.922	1.118	2.207	49.0	138.4	91.8
Min2	Triplet	1.543	3.022	1.117	2.214	44.9	143.5	105.7
TS	Quintet	1.825	1.959	1.123	2.192	70.7	124.8	57.5
TS	Triplet	1.731	1.467	1.152	1.978	75.9	134.5	46.0

> 7400 cm^{-1}. The V$^+$−OCO stretching frequency in this band is observed to be 107 cm^{-1}, significantly lower than for the ground state (210 cm^{-1}), consistent with the calculations. Figure 7 shows that at the V$^+$−C bond length in the ground state, the ligand rotates to reduce the V$^+$−O repulsion. The nearly flat rocking potential calculated for these states is consistent with a 25 cm^{-1} vibrational progression observed in

the photodissociation spectrum and tentatively assigned to the metal-ligand rock.[1] The highest-energy quintet state shown correlates to V$^+$ (^5P, $3d^34s$), and it is the state observed in the visible, near 15 800 cm^{-1}. As expected from the electron configuration, its V$^+$−OCO stretching and bending potentials are similar to those of the near-IR states. The equilibrium V−O bond length is ≈2.45 Å. At the V$^+$−C bond
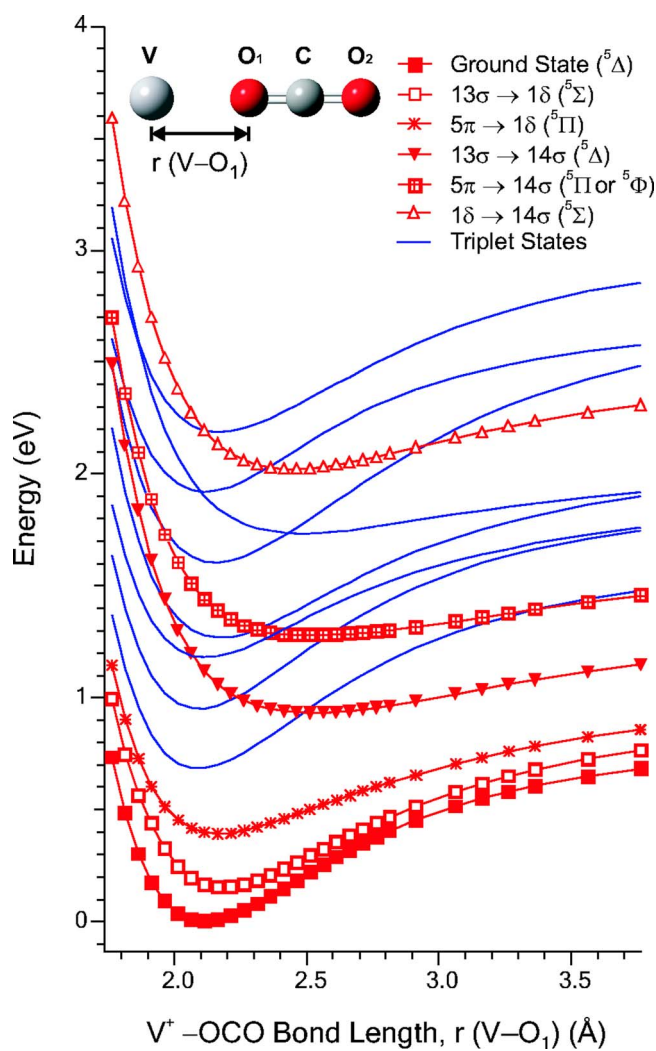

FIG. 6. (Color online) Adiabatic potential energy curves along the V$^+$−(OCO) stretch from TD-DFT calculations at the BHandHLYP/6-311 +G(3df) level. Quintet states are shown with lines and symbols and triplet states with lines. At each V$^+$−(OCO) distance, r(V−O$_1$), all other bond lengths are optimized for the ground state of the linear complex, for each spin state.
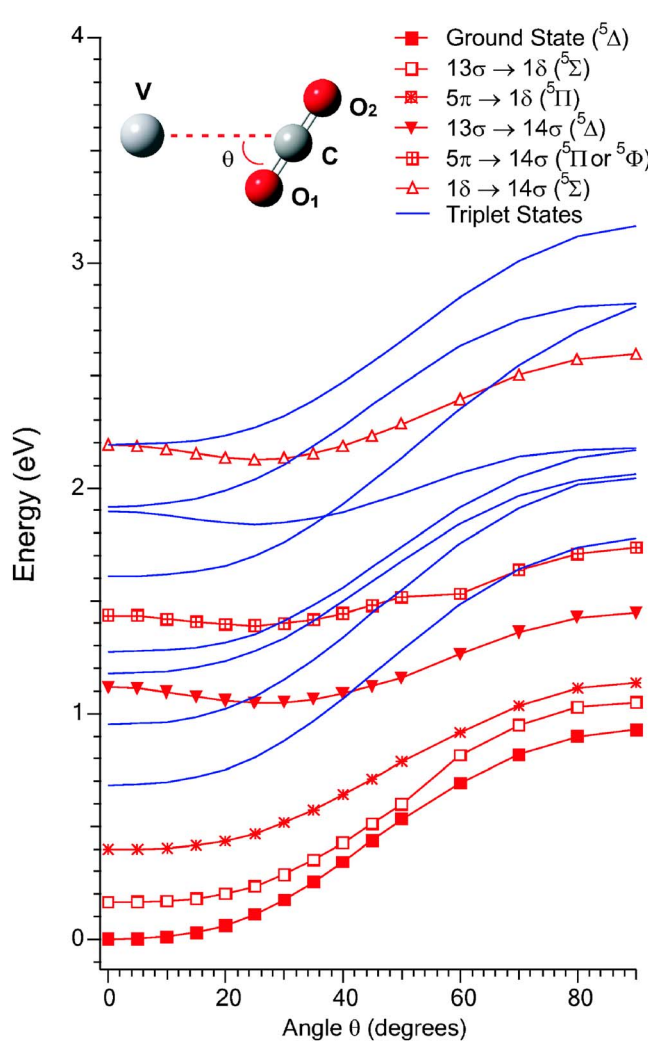
FIG. 7. (Color online) Potential energy curves along the rocking coordinate for V$^+$(OCO). Quintet states are shown with lines and symbols and triplet states with lines. As the V−O$_1$−C angle (θ) is scanned from 0° to 90°, the V−C bond length and the geometry of the OCO ligand are fixed at their values at the quintet minimum.

length of the ground state, the ligand also rotates away from linearity. This is consistent with the observation of progressions in the V$^+$–OCO stretch (186 cm^{-1}) and rock (105 cm^{-1}) in the photodissociation spectrum. Overall, the TD-DFT calculations of the quintet states of V$^+$(OCO) do an excellent job of predicting the observed photodissociation spectrum. Modeling the dissociation dynamics, in which VO$^+$ ($^3\Sigma$)+CO is a major product, requires characterizing triplet states of V$^+$(OCO) and their coupling to the quintet states.

The lowest triplet state of V$^+$ is ^3F ($3d^34s$), which is calculated to lie 0.56 eV above the quintet ground state, and there are several excited triplet states that lie nearby, including one other $3d^34s$ state and four $3d^4$ states within about 1 eV.[35] The short bond lengths and linear minima for the lowest triplet states of V$^+$(OCO) suggest that these states arise from $3d^4$ configurations of V$^+$. As shown in Figs. 6 and 7, calculations predict that there are several triplet states that lie near (and even cross) the excited quintet states. Because several triplet states at similar energies are involved, we expect this general picture to be correct, despite the limited accuracy of TD-DFT calculations.

Dissociation of excited quintet states of V$^+$(OCO) to produce VO$^+$(^3F)+CO($^1\Sigma$) requires spin-orbit coupling of quintet states to triplet states. Calculations by Rue *et al.* looked at coupling between quintet and triplet states of the isoelectronic V$^+$(CS$_2$) system.[36] They argued that the main contribution to the spin-orbit coupling is from the heavy atoms and used calculations on VS$^+$ to estimate the spin-orbit coupling in V$^+$(CS$_2$). To estimate the spin-orbit coupling, calculations were carried out for VO$^+$ at several different bond lengths, and for V$^+$(OCO) at the Min1 triplet geometry. The GAMESS (Refs. 37 and 38) package was used for the spin-orbit calculations.[39] The calculations consist of a restricted open-shell Hartree-Fock calculation on the triplet state, using the 6-31G basis set on all atoms. The lowest triplet and quintet states are calculated separately using the complete active space (CASSCF) method, with an active space consisting of the 4s and 3d on vanadium and 2s and 2p on oxygen. Excited quintet and triplet states are calculated using configuration interaction (CI) based on the CASSCF states.[40] Spin-orbit coupling between the CI states is calculated using the full two-electron Pauli-Breit operator, with effective nuclear charges Z_{eff}=10.5, 6.0, and 3.9 for V, O, and C, respectively.[36]

Calculated coupling between excited quintet and triplet states ranges from ~10 to ~90 cm^{-1} for VO$^+$ at r=1.543 Å, decreasing slightly to ~10 to ~70 cm^{-1} at 2.096 Å, where the range given reflects the fact that different excited triplet states have differing couplings. Calculations at 2.096 Å using the larger 6-311+G(3df) basis set on all atoms give slightly lower couplings of ~10–65 cm^{-1}. All calculations on V$^+$(OCO) were carried out at the optimized Min1 triplet geometry, which has r(V-O$_1$)=2.096 Å. This is very similar to the Min1 quintet geometry. The active space consists of the 4π, 5π, 13σ, 1δ, and 14σ molecular orbitals, as shown in Fig. 4. Spin-orbit couplings between excited quintet and triplet states are calculated to be ~10–140 cm^{-1} with the 6-31G basis and ~10–90 cm^{-1} with the 6-311

+G(3df) basis. At the same V-O bond length, the calculations predict slightly larger spin-orbit coupling for V$^+$(OCO) than for VO$^+$, although this may be due to using different active spaces in the two cases.

Our results show that spin-orbit coupling in V$^+$(OCO) is slightly larger than for VS$^+$ (~20 cm^{-1}),[36] but is still weak for most states and moderate[41] for a few states. This helps to explain why collisional excitation[31] of V$^+$(OCO) leads to V$^+$+CO$_2$ rather than spin-forbidden VO$^+$+CO. Collisional excitation gives a statistical distribution of states.[42] At moderate total energies, the vibrational densities of states in the ground and low-lying quintet states are much higher than in the triplet state, which lies at significantly higher energy. So, low- and moderate-energy collisional excitation should overwhelmingly produce quintet V$^+$(OCO). For quintet V$^+$(OCO), breaking the weak V$^+$–OCO bond is spin allowed and has a loose transition state. In contrast, producing VO$^+$ ($^3\Sigma$) requires intersystem crossing to the triplet state, followed by isomerization over a tight transition state (Fig. 5). A small amount of VO$^+$ is observed at collision energies over 8 eV, comprising 3% of the product at 20 eV. This may be due to production of *quintet* VO$^+$ ($^5\Sigma$)+CO, which lies 3.5 eV above V$^+$(OCO), based on our calculation.

Photodissociation of V$^+$(OCO) in the near-IR produces only V$^+$. This is likely because the lowest transition state to insertion is calculated to lie 1.61 eV (12 985 cm^{-1}) above quintet V$^+$(OCO), which is significantly higher than the 6050–7450 cm^{-1} excitation energy for the near-IR band.[1]

In contrast, photoexcitation of V$^+$(OCO) in the visible produces electronically excited quintet state molecules which survive for many vibrational and even rotational periods, as evidenced by the clearly resolved structure in the photodissociation spectrum. Several vibrational features are <3.5 cm^{-1} wide, with unresolved rotational structure contributing to this width, indicating lifetimes of >1.4 ps. The slow internal conversion permits nonstatistical dynamics, which lead to the observed mode selectivity.

We can use a simple model to estimate the branching ratio between the reactive and nonreactive channels. The initially photoexcited quintet V$^+$(OCO) can undergo internal conversion, producing vibrationally excited, lower-lying quintet states, or, via intersystem crossing (ISC), it can form triplet states. On the lowest quintet surface, production of V$^+$+CO$_2$ is favored, as it occurs over a lower barrier and via a loose transition state. On the lowest triplet surface, the reactive and nonreactive channels have similar barriers. In this simple model, if an initially excited state has a large intersystem crossing rate k_{ISC}, then it is more likely to form the reactive VO$^+$ product. We can calculate, approximately, the intersystem crossing rate k_{ISC} using the "Golden Rule" expression[43]

$$k_{ISC} = \frac{2\pi}{\hbar} v_{ISC}^2 \rho_f(E),$$

where $\rho_f(E)$ is the density of states in the final (triplet) state at energy E and we assume that direct spin-orbit coupling dominates the intersystem crossing rate, so

$$v_{ISC} = \langle \psi_3 | H_{SO} | \psi_5 \rangle \langle \chi_3 | \chi_5 \rangle.$$

The first term is the spin-orbit coupling constant which we calculated, and we ignore the variation of spin-orbit coupling with geometry. The second term is the overlap of the initially excited quintet state vibrational wavefunction with each triplet vibrational state at nearby energy. This term is responsible for the mode selectivity in the intersystem crossing rate, and hence in the photodissociation. Calculated k_{ISC} are convoluted with a 100 cm^{-1} full width at half maximum (FWHM) Lorentzian to average over uncertainties in relative energies due to vibrational anharmonicity and the relative energies of the quintet and triplet states. To compute the vibrational overlap integral, we assume that the vibrations are harmonic and separable; the multidimensional overlap integral is then the product of one-dimensional overlaps along each vibration. All vibrations are included; the vibrational frequencies for the excited quintet state are the experimental values,[1] the frequencies for the triplet state are assumed to be those calculated for the lowest triplet state at the B3LYP/6-311+G(d) level. Displacements along each normal mode are estimated as follows: the displacements between the ground and excited quintet state are calculated by matching observed intensities in the photodissociation spectrum (Fig. 2) and the displacement between the ground quintet state and the excited triplet state is assumed to be small (see below). From the spectrum, there is substantial displacement in the V$^+$–OCO stretch, with smaller displacements in the bend and rock, and very little displacement in the OCO stretches. The observed progressions in the bend and rock, as well as Fig. 7, indicate that there is coupling between the V$^+$–OCO stretch and these vibrations, as the minimum energy geometries of the ground and excited quintet states are both calculated to be linear.

The initially excited quintet state can couple to several triplet states. The minimum in the lowest triplet state of V$^+$(OCO) lies ~11 000 cm^{-1} below the minimum of the initially excited state and has a similar geometry to the ground quintet state, as shown in Figs. 6 and 7. As a result of the large energy gap and modest difference in geometry, the vibrational overlap integrals and k_{ISC} are calculated to be very small. The vibrational overlaps are only substantial for states within ~2500 cm^{-1} of the initially excited state. This is consistent with Fig. 2, which shows a Franck-Condon envelope that extends for ~1400 cm^{-1} for the transition between the ground and excited quintet states; calculated overlaps between excited triplet states and the excited quintet states should show a similar range, as the excited triplet states have similar geometries to the ground quintet state. For a triplet state 2500 cm^{-1} below the quintet state, and assuming a spin-orbit coupling constant of 50 cm^{-1}, $k_{ISC} \approx 10^8$ s^{-1}. Parameters used to calculate k_{ISC} are given in Table S3 of Ref. 8. Excitation in the V$^+$–OCO stretch, ν'_3 increases the rate, especially for several quanta. The displacement between the excited quintet and triplet states is mostly along the V$^+$–OCO stretch, so it is not surprising that excitation in this vibration enhances the vibrational overlap and promotes intersystem crossing.

Several trends in the calculated k_{ISC} (listed in Table S1 of

Ref. 8) agree with our observations of the branching ratio. In general, more quanta of ν'_3 increase the yield of the reactive channel. This is not simply the result of increasing energy, as the state with one quantum of OCO bend, ν'_4 is observed and calculated to be substantially less reactive than $3\nu'_3$ and $3\nu'_3 + \nu'_5$, which bracket its energy. Exciting the OCO antisymmetric stretch ν'_1 is also calculated to increase k_{ISC}, especially when combined with exciting ν'_3, in accord with experiment. This is due to two effects. The density of states increases with energy, and exciting ν'_1 (especially in combination with ν'_3) increases the vibrational overlap.

The calculations do not reproduce all of the experimental observations. First, the calculations predict that exciting *any* vibration enhances the reactivity. Experimentally, states with one quantum of ν'_3 and one quantum of ν'_4 are less reactive than the vibrational ground state. Also, the calculations predict large enhancements in k_{ISC}, by a factor of ~40 for states with several quanta of ν'_3 and by a factor of ~120 for these states in combination with ν'_1. This is much larger than the observed range of reactivities. Also, the calculations predict mode selectivity for quite highly vibrationally excited states, while, experimentally, states at higher energies tend to have similar reactivities. There are several possible reasons for these discrepancies. First, it is possible, by chance, for the initially excited vibrational state to be nearly in resonance with a state with good vibrational overlap. This leads to large variations in calculated k_{ISC}, especially at low energies, where the density of states of the triplet state is modest. In the calculations, we smooth this out somewhat by averaging calculated k_{ISC} over a 100 cm^{-1} FWHM Lorentzian. This may, however, explain the surprisingly low observed reactivity of ν'_3—there may just happen to be few triplet vibrational states at nearby energies. Vibrational mixing in the excited quintet state, due to cross anharmonicity and intramolecular vibrational distribution, may help to explain why there is less mode selectivity observed at higher energies, as the initially excited state may not be very pure. The overestimate of mode selectivity in the calculations may also be due to not considering intersystem crossing to other triplet states, as well as to ignoring the effect of initially excited state on the internal conversion rate, and not considering the competition between production of VO$^+$ and V$^+$ in the triplet manifold.

Photodissociation of V$^+$(OCO) in the visible is mode selective, with excitation of the V$^+$–OCO stretch and, to a lesser extent, V$^+$–OCO rock and OCO antisymmetric stretch enhancing the yield of the reactive VO$^+$ channel. The mechanism for this enhancement is fairly complex, as the calculations predict that producing VO$^+$ requires intersystem crossing to the triplet surface, and the transition state to produce VO$^+$ is not linear. The V$^+$–OCO stretch and OCO antisymmetric stretch appear to enhance reactivity by increasing the intersystem crossing rate, while the rock may increase the VO$^+$ yield on the triplet surface.

[1] M. Citir, G. Altinay, and R. B. Metz, J. Phys. Chem. A **110**, 5051 (2006).

[2] M. Sodupe, V. Branchadell, M. Rosi, and C. W. Bauschlicher, Jr., J. Phys. Chem. A **101**, 7854 (1997).

[3] D. E. Lessen, R. L. Asher, and P. J. Brucat, J. Chem. Phys. **95**, 1414 (1991).

[4] J. Husband, F. Aguirre, P. Ferguson, and R. B. Metz, J. Chem. Phys. **111**, 1433 (1999).

[5] R. B. Metz, Int. Rev. Phys. Chem. **23**, 79 (2004); Adv. Chem. Phys. **138**, 331 (2008).

[6] L. S. Rothman, D. Jacquemart, A. Barbe *et al.*, J. Quant. Spectrosc. Radiat. Transf. **96**, 139 (2005).

[7] S. Gerstenkorn and P. Luc, *Atlas du Spectre D'Absorption de la Molecule D'Iode* 14 800–20 000 cm^{-1} (Editions du Centre National de la Recherche Scientifique, Paris, 1978).

[8] See EPAPS Document No. E-JCPSA6-127-013747 for Table S1: positions, assignments, VO$^+$/V$^+$ branching ratios, and calculated intersystem crossing rates for one photon and vibrationally mediated photodissociation of V$^+$(OCO); Table S2: calculated energies for V$^+$ electronic states from TD-DFT calculations; and Table S3: parameters used for intersystem crossing rate calculations. This document can be reached through a direct link in the online article's HTML reference section or via the EPAPS homepage (http://www.aip.org/pubservs/epaps.html).

[9] F. F. Crim, Annu. Rev. Phys. Chem. **44**, 397 (1993).

[10] I. Bar and S. Rosenwaks, Int. Rev. Phys. Chem. **20**, 711 (2001).

[11] C. Tao and P. J. Dagdigian, Chem. Phys. Lett. **350**, 63 (2001).

[12] O. Votava, D. F. Plusquellic, and D. J. Nesbitt, J. Chem. Phys. **110**, 8564 (1999).

[13] A. D. Becke, J. Chem. Phys. **98**, 5648 (1993).

[14] C. Lee, W. Yang, and R. G. Parr, Phys. Rev. B **37**, 785 (1988).

[15] B. Miehlich, A. Savin, H. Stoll, and H. Preuss, Chem. Phys. Lett. **157**, 200 (1989).

[16] J. A. Pople, M. Head-Gordon, and K. Raghavachari, J. Chem. Phys. **87**, 5968 (1987).

[17] C. Peng, P. Y. Ayala, H. B. Schlegel, and M. J. Frisch, J. Comput. Chem. **17**, 49 (1996).

[18] C. Peng and H. B. Schlegel, Isr. J. Chem. **33**, 449 (1994).

[19] M. J. Frisch, G. W. Trucks, H. B. Schlegel *et al.*, GAUSSIAN 03, Revision C.02, Gaussian, Inc., Wallingford, CT, 2004.

[20] J. Harrington and J. C. Weisshar, J. Chem. Phys. **97**, 2809 (1992).

[21] E. Sicilia and N. Russo, J. Am. Chem. Soc. **124**, 1471 (2002).

[22] M. Pykavy and C. vanWüllen, J. Phys. Chem. A **107**, 5566 (2003).

[23] M. Calatayud, B. Silvi, J. Andrés, and A. Beltrán, Chem. Phys. Lett. **333**, 493 (2001).

[24] J. F. Harrison, Chem. Rev. (Washington, D.C.) **100**, 679 (2000).

[25] Y. Nakao, K. Hirao, and T. Taketsugu, J. Chem. Phys. **114**, 7935 (2001).

[26] D. Schröder, M. Engeser, H. Schwarz, and J. N. Harvey, ChemPhysChem **3**, 584 (2002).

[27] P. B. Armentrout and B. L. Kickel, in *Organometallic Ion Chemistry*, edited by B. S. Freiser (Kluwer, Dordrecht, 1996).

[28] D. E. Clemmer, N. Aristov, and P. B. Armentrout, J. Phys. Chem. **97**, 544 (1993).

[29] D. E. Clemmer, J. L. Elkind, N. Aristov, and P. B. Armentrout, J. Chem. Phys. **95**, 3387 (1991).

[30] G. Balducci, G. Gigli, and M. Guido, J. Chem. Phys. **79**, 5623 (1983).

[31] M. R. Sievers and P. B. Armentrout, J. Chem. Phys. **102**, 754 (1995).

[32] G. K. Koyanagi and D. K. Bohme, J. Phys. Chem. A **110**, 1232 (2006).

[33] F. Aguirre, J. Husband, C. J. Thompson, K. L. Stringer, and R. B. Metz, J. Chem. Phys. **119**, 10194 (2003).

[34] E. Broclawik and T. Borowski, Chem. Phys. Lett. **339**, 433 (2001).

[35] J. Sugar and C. Corliss, J. Phys. Chem. Ref. Data **14**, 1 (1985).

[36] C. Rue, P. B. Armentrout, I. Kretzschmar, D. Schröder, J. N. Harvey, and H. Schwarz, J. Chem. Phys. **110**, 7858 (1999).

[37] M. W. Schmidt, K. K. Baldridge, J. A. Boatz *et al.*, J. Comput. Chem. **14**, 1347 (1993).

[38] M. S. Gordon and M. W. Schmidt, in *Theory and Applications of Computational Chemistry, the First Forty Years*, edited by C. E. Dykstra, G. Frenking, K. S. Kim, and G. E. Scuseria (Elsevier, Amsterdam, 2005).

[39] D. G. Fedorov, S. Koseki, M. W. Schmidt, and M. S. Gordon, Int. Rev. Phys. Chem. **22**, 551 (2003).

[40] M. W. Schmidt and M. S. Gordon, Annu. Rev. Phys. Chem. **49**, 233 (1998).

[41] G. E. Zahr, R. K. Preston, and W. H. Miller, J. Chem. Phys. **62**, 1127 (1975).

[42] M. T. Rodgers, K. M. Ervin, and P. B. Armentrout, J. Chem. Phys. **106**, 4499 (1997).

[43] P. Avouris, W. M. Gelbart, and M. A. El-Sayed, Chem. Rev. (Washington, D.C.) **77**, 793 (1977).